Circulation times of hepatocellular carcinoma cells by *in vivo* flow cytometry

Yan Li (李 延)[1,2], Zhichao Fan (樊志超)[1,2], Jin Guo (郭 进)[1,2], Guangda Liu (刘光大)[2,3], Xiaoying Tan (谭晓英)[1,2], Cheng Wang (王 成)[4], Zhengqin Gu (顾正勤)[5], and Xunbin Wei (魏勋斌)[1,2*]

[1]*Department of Chemistry, Fudan University, Shanghai 200433, China*

[2]*Institutes of Biomedical Sciences, Fudan University, Shanghai 200032, China*

[3]*Shanghai Medical College, Fudan University, Shanghai 200032, China*

[4]*School of Medical Instrument and Food Engineering, University of Shanghai for Science and Technology, Shanghai 200093, China*

[5]*Department of Urology, Xinhua Hospital, Shanghai Jiaotong University, Shanghai 200092, China*

[*]*E-mail: xwei@fudan.edu.cn*

Received July 7, 2010

Hepatocellular carcinoma (HCC) may metastasize to many organs. The survival rate is almost zero for metastatic HCC patients. Molecular mechanisms of HCC metastasis need to be understood better and new therapies must be developed. We have developed the "*in vivo* microscopy" to study the mechanisms that govern liver tumor cells spreading through the microenvironment *in vivo*. A recently developed "*in vivo* flow cytometer" combined with real-time confocal fluorescence imaging is used to assess spreading and the circulation kinetics of liver tumor cells. We measure the depletion kinetics of two related human HCC cell lines, high-metastatic HCCLM3 cells and low-metastatic HepG2 cells, which are from the same origin and obtained by repetitive screenings in mice. More than 60% of the HCCLM3 cells are depleted within the first hour. Interestingly, the low-metastatic HepG2 cells possess noticeably slower depletion kinetics. In comparison, less than 40% of the HepG2 cells are depleted within the first hour. The differences in depletion kinetics might provide insights into early metastasis processes.

OCIS codes: 170.0170, 170.3880, 170.4580.

doi: 10.3788/COL20100810.0953.

Metastasis is a very complicated process that still has not been completely understood. In metastasis, the cancer cells that travel through the body are capable of establishing new tumors in locations remote from the site of the original disease. To metastasize, a cancer cell must break away from its tumor and invade either the circulatory or lymph system, which will carry it to a new location and establish itself in the new site[1]. The body has many safeguards to prevent cells from doing this, yet many cancer cells have the ability to overcome these safeguards. Research is now focused on understanding in what ways cancer cells have mutated to circumvent the body's defenses and travel to other locations. We have applied "*in vivo* flow cytometry" to study the mechanisms that govern the early steps in liver tumor cells spreading through the microenvironment.

The growth of tumor need blood supply as healthy cells do. This access allows detached malignant cells from the tumor to enter the bodies' general bloodstream[1−3]. Once in the blood stream, the cancer cells have access to every portion of the body. The lymphatic system has its own channels throughout the body like the circulatory system, through which a malignant cell can travel. The cancer cell in the bloodstream must fight the body's defense system and try to re-attach itself in a new location. Fewer than 1 in 10000 cancer cells survive circulation to create a new tumor. The circulation of the blood plays a significant role in determining where cancer cells travel. The cancer cells usually get trapped in the first set of capillaries they encounter downstream from their point of entry. Frequently these capillaries are in the lungs, since returning deoxygenated venous blood leaving many organs is returned to the lungs for reoxygenation. From the intestines, the blood goes to the liver first, so cancer cells leaving the intestines will go there. The lungs and the liver are the two most common sites for metastasis in the human body. Many circulating cancer cells can not finish the entire process of metastasis[4]. Properties in the tumor itself, such as deformability, aggregation, and expression of adhesive molecules, cause the deaths[5−13].

Liver cancer is one of the most common malignancies in the world, with approximately a million cases reported every year. Although two-thirds of people have advanced liver disease when they seek medical help, one-third of the patients have cancer that has not progressed beyond the liver. The most promising treatments apply to this latter group. Primary liver cancer (hepatocellular carcinoma, or HCC) is associated with liver cirrhosis 60%−80% of the time.

HCC may metastasize to lung, bones, kidney, and many other organs[14−18]. Surgical resection, liver transplantation, chemotherapy, and radiation therapy are the foundation of current HCC therapies. However, the outcomes are poor: the survival rate is almost zero for metastatic HCC patients. Molecular mechanisms of HCC metastasis need to be understood better and new therapies must be developed to selectively target to unique characteristics of HCC cell growth and metastasis.

Optical techniques should open a new window to study the molecular mechanisms of cancer and cancer metastasis. Previously, researchers have used a number of optical methods to study HCC and other cancer[19−21]. Here we use the "*in vivo* flow cytometry" combined with optical imaging to study early HCC metastasis.

The *in vivo* flow cytometer has the capability to detect and quantify continuously the number and flow characteristics of fluorescently labeled cells *in vivo*[22−28]. The *in vivo* flow cytometer allows researchers to acquire cytometric information from the circulation in live animals without extracting blood sample (Fig. 1). Previous researchers demonstrate that using this technique, the number of fluorescently labeled circulating cells can be quantified in a real-time and reproducible manner in live animal. We set up our *in vivo* flow cytometer to detect fluorescence signal from a given circulating tumor cell (CTC) population in a confocal geometry based on previous groups' experiences[22,23]. Briefly, fluorescence signal from a given circulating cell population is recorded as the cells pass through the slit of light. Confocal detection of the excited fluorescence enables continuous monitoring of labeled cells in the upper layers of scattering tissue, such as the skin of a mouse ear. The size of the slit at the focal plane of the sample is approximately 5×72 (μm). The depth of focus (i.e., the full-width at half-maximum (FWHM) of the light slit onto the sample in the axial direction) is approximately 50 μm, a value chosen to match the vessels of interest. The sample is positioned so that the long dimension of the slit traverses the width of the blood vessel; thus, fluorescence is excited as the labeled cells in circulation pass through the slit. Fluorescence is detected with a photomultiplier tube placed directly behind the mechanical slit, sampled at a rate of 5 kHz with a data acquisition card, and displayed and stored in a computer. The device is used to characterize the *in vivo* kinetics of red and white blood cells circulating in the mouse ear vasculature, as well as in the circulating liver cancer cells.

In experiments, the BALB/c nude mice were anesthetized and injected intravenously with DiD-fluorescently-labeled HCCLM3 human liver tumor cells. HCCLM3 is a HCC cell line with high metastatic potential and is comparatively easier to metastasize to the lung in BALB/c nude mice than other cell lines[29]. Studying the depletion kinetics of HCCLM3 cells in the circulation could help understanding the early metastatic process. After the injection, mice were placed on a heated stage and an artery in the ear was chosen for measurements. Fluorescence signal was excited as the labeled circulating cells passed through a laser slit focused across the blood vessel (Fig. 2). Detecting the excited fluorescence confocally enables researchers to monitor labeled cells in the animal circulation system continuously. Signal was recorded at a rapid rate (5 kHz) to ensure the measurement of fast-flowing cells (Fig. 3). The number of

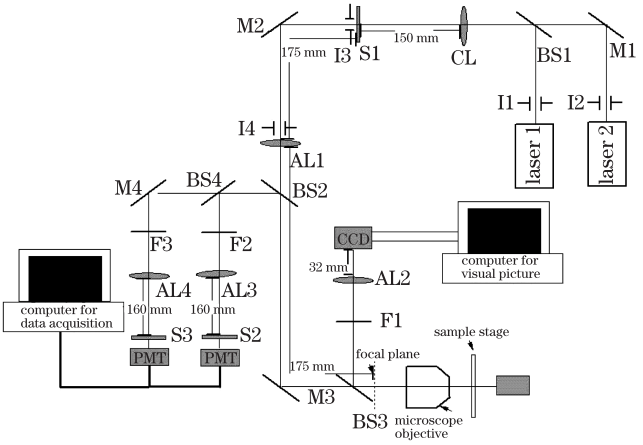

Fig. 1. Schematic of the two-color *in vivo* flow cytometer experimental setup. Laser light (488 or 635 nm) is focused into a slit by a cylindrical lens (CL) and imaged across the selected blood vessel with a microscope objective lens (40×, numerical aperture NA=0.6). The fluorescence is collected by the same microscope objective, directed through the dichroic beam splitter BS3 (reflection 25%, transmission 75%, Edmund Optics), reflected by a mirror, a second splitter BS2 (transmission $\geq$ 90% for 488 and 635 nm; reflection $\geq$ 90% for 499–622 and 652–755 nm, Semrock) and a third dichroic beam splitter BS4 (edge wavelength 516 nm, reflection band >90% for 490–510 nm, transmission band >90% for 520–700 nm, Semrock), and imaged onto a 200×3000 (μm) mechanical slit, which is confocal with the excitation slit. F1–F3: bandpass filter (F1: 509–552 nm; F2: 500–520 nm; F3: 640–690 nm; Semrock); BS1: beam splitter (edge wavelength 505 nm, reflection band 513–725 nm, transmission band 446–500 nm, Semrock); AL1–AL4: achromats; I1–I4: irises; PMT: photomultiplier tube; LED: light-emitting diode.

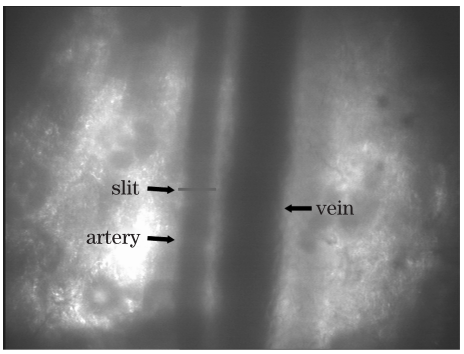

Fig. 2. The mouse is anesthetized and placed on a heated stage. An artery is chosen in the ear for the measurement. The fluorescence signal from DiD-labeled circulating cells is recorded when the cells pass through a slit of light focused across the artery. DiD is a fluorescence dye to label the membrane lipid (excitation peak: 640 nm; emission peak: 660–670 nm; Molecular Probes).

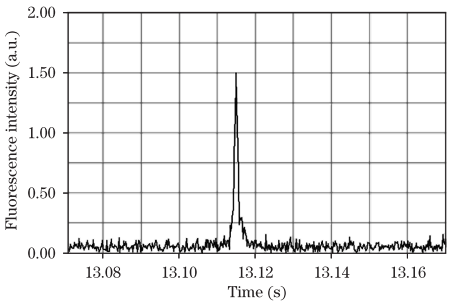

Fig. 3. A trace of labeled circulating HCCLM3 hepatocellular carcinoma cell measured by the *in vivo* flow cytometer, after intravenously introduced into a mouse. The peak within the trace indicates that a DiD-labeled HCCLM3 cell passes through the slit of light and thus gives a burst of fluorescence.

fluorescent peaks, along with the height and FWHM of each peak, was determined using algorithms developed by ourselves. The device has been used to characterize the *in vivo* kinetics of red and white blood cells circulating in the mouse ear vasculature as well as the circulating prostate cancer cells[9,22−25].

The sample isolation and preparation steps here are bypassed altogether in contrast to the measurement of a typical conventional (*in vitro*) flow cytometer. Multiple measurements in the *in vivo* flow cytometer are carried out noninvasively. We have measured the depletion kinetics of two related human HCC cell lines, high-metastatic HCCLM3 cells and low-metastatic HepG2 cells, which were from the same HCC patient and obtained by repetitive screenings in mice[29].

The depletion kinetics of circulating HCCLM3 cells in BALB/c nude mice during the first 12 h following injection of the fluorescently labeled cells illustrates the depletion process (Fig. 4). More than 60% of the cells are depleted within the first hour. After the initial depletion, there is a re-appearance in the number of circulating cells, quickly followed by a second depletion. This phenomenon was also observed in previous study on prostate cancer cells[9]. By 12 h, about 94% HCCLM3 cells are depleted from the circulation. Interestingly, the low-metastatic HepG2 cells possess noticeably slower depletion kinetics. In comparison, less than 40% of the HepG2 cells are depleted within the first hour. By 12 h, about 55% of the HepG2 cells are depleted from the circulation. When present in circulation for extensively long time, cancer cell might undergo cell death due to the lack of survival signal from cell adhesion and the harsh environment imparted by the sheer stress[6,30]. Therefore, the differences in depletion kinetics might provide insights into early metastasis processes.

The *in vivo* flow cytometry is particularly useful for studying small animal models of tumors. For example, it is often difficult to obtain sufficient blood volume from a single mouse, whose total blood volume is only about 2 ml. This is particularly true when multiple blood samples are needed. With this *in vivo* technique, multiple measurements can be performed on a single animal over time, minimizing the number of animals and also eliminating variation between individuals.

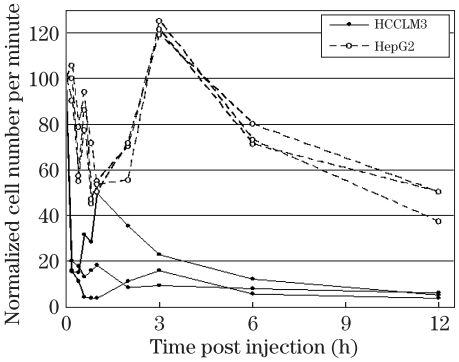

Fig. 4. Depletion kinetics of circulating high-metastatic HCCLM3 cells and low-metastatic HepG2 cells in BALB/c nude mice. The normalized numbers of circulating cells per minute are shown for 12 h following injection of the DiD-fluorescently-labeled cells to illustrate the depletion process. More than 60% of the HCCLM3 cells are depleted within the first hour. By 12 h, about 94% of the HCCLM3 cells are depleted from the circulation. In comparison, the low-metastatic HepG2 cells possess noticeably slower depletion kinetics. Less than 40% of the HepG2 cells are depleted within the first hour. By 12 h, about 55% of the HepG2 cells are depleted from the circulation.

Detection of green fluorescence signal on CTCs could be technically more difficult. It is particularly true for detection through blood because of the strong absorption below about 590 nm[31,32]. Both excitation and emission will be attenuated respectively on the way in and on the way out. It might be a potential problem for *in vivo* flow cytometer to pick up the green fluorescence signal on circulating cells, depending on the green fluorescence level, although we have detected green fluorescence signal from different cell populations in circulation (unpublished results). One method to enhance the sensitivity is to utilize the multi-photon detection, although with significantly higher cost. A multi-photon intravital flow cytometer to quantifity rare CTCs *in vivo* has been developed and moderately higher sensitivity than confocal detection used in our current *in vivo* flow cytometer has been achieved[27,31−35]. Another method is to use the photothermal/photoacoustic detection, which also improves the detection depth. Zharov *et al.* developed a photothermal image flow cytometer to detect target cells in blood and lymph flow *in vivo*[36−38]. They used nanoparticles to enrich the rare cells and achieved significantly higher sensitivity[39−41].

The study here focuses on measuring circulating liver tumor cells. However, the methods developed here should be applicable to various potential biomarkers in circulation for detecting cancer, characterizing pathologic malignant tumors, assessing disease prognosis, and predicting and measuring response to treatments, thus providing invaluable information about detecting and treating cancer. Furthermore, the developed methods will be useful to monitor the circulating cells in general.

We thank Charles P. Lin for collaboration. We also thank Guiying Wang, Zenghui Zhou, and Li Wang for helpful discussions. Yan Li and Zhichao Fan contribute equally to this letter. This work was partially supported by the National "973" Program of China (No. 2011CB910400), the China National Key Projects for Infectious Disease (No. 2008ZX10002-021), the National Science Foundation of China (Nos. 30770524 and 20975027), the Ministry of Education of China (No. 109056), "Shuguang Scholarship" from the Education Commission of Shanghai Municipality, and the Program for New Century Excellent Talents in University Award (NCET-08-0131).

References

1. E. Bedner, H. D. Halicka, W. Cheng, T. Salomon, A. Deptala, W. Gorczyca, M. R. Melamed, and Z. Darzynkiewicz, Cytometry **36,** 77 (1999).
2. F. G. Blankenberg, L. Naumovski, J. F. Tait, A. M. Post, and H. W. Strauss, J. Nucl. Medicine **42,** 309 (2001).
3. T. Aotake, C. D. Lu, Y. Chiba, R. Muraoka, and N. Tanigawa, Clin. Cancer Res. **5,** 135 (1999).
4. F. Durrieu, F. Belloc, L. Lacoste, P. Dumain, J. Chabrol, J. Dachary-Prigent, H. Morjani, M. R. Boisseau, J. Reiffers, P. Bernard, and F. Lacombe, Exp. Cell Res. **240,**

165 (1998).
5. O. Ek, G. H. Reaman, D. L. Crankshaw, L. M. Chelstrom, D. E. Myers, and F. M. Uckun, Leuk. Lymphoma **28,** 509 (1998).
6. N. Gaiano, J. S. Nye, and G. Fishell, Neuron **26,** 395 (2000).
7. N. Gaiano, J. D. Kohtz, D. H. Turnbull, and G. Fishell, Nature Neurosci. **2,** 812 (1999).
8. B. Fadeel, S. Orrenius, and B. Zhivotovsky, Biochem. Biophys. Res. Commun. **266,** 699 (1999).
9. I. Georgakoudi, N. Solban, J. Novak, W. L. Rice, X. Wei, T. Hasan, and C. P. Lin, Cancer Res. **64,** 5044 (2004).
10. H. R. Herschman, Science **302,** 605 (2003).
11. S. Holdenrieder and P. Stieber, Clin. Biochem. **37,** 605 (2004).
12. S. Jahr, H. Hentze, S. Englisch, D. Hardt, F. O. Fackelmayer, R. D. Hesch, and R. Knippers, Cancer Res. **61,** 1659 (2001).
13. B. Laxman, D. E. Hall, M. S. Bhojani, D. A. Hamstra, T. L. Chenevert, B. D. Ross, and A. Rehemtulla, PNAS **99,** 16551 (2002).
14. T. F. Massoud and S. S. Gambhir, Genes Development **17,** 545 (2003).
15. S. Nery, H. Wichterle, and G. Fishell, Development **128,** 527 (2001).
16. V. Ntziachristos, E. A. Schellenberger, J. Ripoll, D. Yessayan, E. Graves, A. Bogdanov, Jr., L. Josephson, and R. Weissleder, PNAS **101,** 12294 (2004).
17. S. Osella-Abate, A. Zaccagna, P. Savoia, P. Quaglino, B. Salomone, and M. G. Bernengo, J. Am. Acad. Dermatol. **44,** 40 (2001).
18. J. C. Reed, J. Clin. Oncol. **17,** 2941 (1999).
19. L. Li, H. Wei, B. He, Z. Guo, H. Yang, S. Xie, X. Chen, L. Li, G. Wu, and J. Lu, Acta Opt. Sin. (in Chinese) **29,** 2860 (2009).
20. J. Li, H. Zeng, and X. Pang, Acta Opt. Sin. (in Chinese) **29,** 2261 (2009).
21. H. Zhang, W. Ma, Z. Zou, W. Gao, Z. Xue, and Y. Li, Chinese J. Lasers (in Chinese) **35,** 631 (2008).
22. J. Novak, I. Georgakoudi, X. Wei, A. Prossin, and C. P. Lin, Opt. Lett. **29,** 77 (2004).
23. S. Boutrus, C. Greiner, D. Hwu, M. Chan, C. Kuperwasser, C. Lin, and I. Georgakoudi, J. Biomed. Opt. **12,** 020507 (2007).
24. D. A. Sipkins, X. Wei, J. W. Wu, J. M. Runnels, D. Cote, T. K. Means, A. D. Luster, D. T. Scadden, and C. P. Lin, Nature **435,** 969 (2005).
25. J. Novak and M. Puoris'haag, Opt. Lett. **32,** 2993 (2007).
26. W. He, H. F. Wang, L. C. Hartmann, J. X. Cheng, and P. S. Low, PNAS **104,** 11760 (2007).
27. C. F. Zhong, E. R. Tkaczyk, T. Thomas, J. Y. Ye, A. Myc, A. U. Bielinska, Z. Cao, I. Majoros, B. Keszler, J. R. Baker, and T. B. Norris, J. Biomed. Opt. **13,** 59801 (2008).
28. Z. Fan, J. A. Spencer, Y. Lu, C. M. Pitsillides, G. Singh, P. Kim, S. H. Yun, V. Toxavidis, T. B. Strom, C. P. Lin, and M. Koulmanda, Nature Medicine **16,** 718 (2010).
29. Y. Li, Z. Y. Tang, S. L. Ye, B. B. Liu, Y. K. Liu, J. Chen, and Q. Xue, J. Cancer Res. Clin. Oncol. **129,** 43 (2003).
30. X. Wei, D. A. Sipkins, C. M. Pitsillides, J. Novak, I. Georgakoudi, and C. P. Lin, Mol. Imaging **4,** 415 (2005).
31. E. R. Tkaczyk, C. F. Zhong, J. Y. Ye, S. Katnik, A. Myc, K. E. Luker, G. D. Luker, J. R. Baker, and T. B. Norris, Proc. SPIE **6631,** 66310T (2007).
32. E. R. Tkaczyk, A. H. Tkaczyk, S. Katnik, J. Y. Ye, K. E. Luker, G. D. Luker, A. Myc, J. R. Baker, and T. B. Norris, J. Biomed. Opt. **13,** 041319 (2008).
33. C. F. Zhong, J. Y. Ye, A. Myc, T. P. Thomas, A. U. Bielinska, J. R. Baker, Jr., and T. B. Norris, Proc. SPIE **5700,** 78 (2005).
34. E. R. Tkaczyk, C. F. Zhong, J. Y. Ye, A. Myc, T. Thomas, Z. Cao, R. Duran-Struuck, K. E. Luker, G. D. Luker, T. B. Norris, and J. R. Baker, Jr., Opt. Commun. **281,** 888 (2008).
35. Y. C. Chang, J. Y. Ye, T. P. Thomas, Z. Cao, A. Kotlyar, E. R. Tkaczyk, J. R. Baker, Jr., and T. B. Norris, J. Biomed. Opt. **15,** 047004 (2010).
36. V. P. Zharov, E. I. Galanzha, and V. V. Tuchin, Opt. Lett. **30,** 628 (2005).
37. V. P. Zharov, E. I. Galanzha, and V. V. Tuchin, J. Cell. Biochem. **97,** 916 (2006).
38. V. P. Zharov, E. I. Galanzha, E. V. Shashkov, N. G. Khlebtsov, and V. V. Tuchin, Opt. Lett. **31,** 3623 (2006).
39. E. I. Galanzha, E. V. Shashkov, V. V. Tuchin, and V. P. Zharov, Cyrometry Part A **73,** 884(2008).
40. E. I. Galanzha, M. S. Kokoska, E. V. Shashkov, J. W. Kim, V. V. Tuchin, and V. P. Zharov, J. Biophoton. **2,** 528 (2009).
41. E. I. Galanzha, E. V. Shashkov, T. Kelly, J. W. Kim, L. Yang, and V. P. Zharov, Nature Nanotechnol. **4,** 855 (2009).